Veronica Natale, Gerhard Stadlmayr, Filippo Benedetti, Katharina Stadlbauer, Florian Rüker and Gordana Wozniak-Knopp*

Trispecific antibodies produced from mAb^2 pairs by controlled Fab-arm exchange

https://doi.org/10.1515/hsz-2021-0376
Received September 28, 2021; accepted January 18, 2022; published online January 31, 2022

Abstract: Bispecific antibodies and antibody fragments are therapeutics of growing importance. They are clinically applied for effector cell engagement, enhanced targeting selectivity, addressing of multiple cellular pathways and active transfer of certain activities into difficult-to-reach compartments. These functionalities could profit from a third antigen specificity. In this work we have employed symmetrical bispecific parental antibodies of mAb^2 format, which feature a novel antigen binding site in the C_H3 domains, and engineered them with a minimal number of point mutations to guide the formation of a controlled Fab-arm exchanged trispecific antibody at a high yield after reduction and re-oxidation. Two model antibodies, one reactive with EGFR, Her2 and VEGF, and one with Fab-arms binding to Ang2 and VEGF and an Fc fragment binding to VEGF, were prepared and examined for heterodimeric status, stability, antigen binding properties and biological activity. Resulting molecules were of good biophysical characteristics and retained antigen reactivity and biological activity of the parental mAb^2 constructs.

Keywords: antigen-binding Fc fragment; EGFR; Her2; heterodimer; multispecific antibodies; VEGF inhibition.

Introduction

In the last two decades, bispecific antibodies have continuously enriched the spectrum of targeted therapies by showing activity in biological situations where their unique property of containing, in one molecule, specificities for two epitopes could surpass the results of single-agent-based approaches. A notable example is their ability to bridge two different cell types and elicit a potent redirection of effector cells to kill target tumor cells (Strohl and Naso 2019), and bispecific antibodies with this mode of action were already approved for clinical use (Newman and Benani 2016). Obligate connection of two specificities in a single molecule has proven invaluable in targeting two receptors on the same cell with the purpose to achieve a superior selectivity and hence superior safety, with such bispecifics working as either antagonists or eliciting an agonistic response (Shi et al. 2018). An enzyme mimetic bispecific antibody, which replaces the missing link in an enzyme cascade by targeting simultaneously Factor IXa and Factor X, was approved for the treatment of hemophilia patients who developed antibodies against Factor VIII (Blair 2019). Finally, antibodies that can mediate their active transfer into otherwise hard-to-reach biological compartments, act as molecular 'Trojan horses' to deliver their activity via a fused biological or their other arm in these milieus (Pardridge 2015), and this mechanism is seen in bispecific antibodies crossing the blood-brain barrier (Kariolis et al. 2020). Even in cases where bispecific antibodies combine the activities that are achievable with the sum of their parts, they can reduce costs in comparison with multiple agents used in combination therapy.

With more than 110 candidates in clinical trials and over 180 molecules in pre-clinical development, bispecific antibodies are bound to make a difference to human health (Labrijn et al. 2019; Nie et al. 2020). But although they are currently only entering the stage of clinical testing, trispecific antibodies appear promising future therapeutics by even extending the unique functionalities of bispecific antibodies. The pioneering example of a trispecific killer cell engager (TriKE) targeting CD16 on natural killer cells and CD33 on target myeloma cells exhibited a more efficient tumor cell killing in a mouse model, when a third

***Corresponding author: Gordana Wozniak-Knopp**, Department of Biotechnology, Christian Doppler Laboratory for Innovative Immunotherapeutics, Institute of Molecular Biotechnology, University of Natural Resources and Life Sciences, Vienna (BOKU), Muthgasse 18, A-1190 Vienna, Austria, E-mail: gordana.wozniak@boku.ac.at. https://orcid.org/0000-0002-4069-070X
Veronica Natale, Gerhard Stadlmayr, Filippo Benedetti, Katharina Stadlbauer and Florian Rüker, Department of Biotechnology, Christian Doppler Laboratory for Innovative Immunotherapeutics, Institute of Molecular Biotechnology, University of Natural Resources and Life Sciences, Vienna (BOKU), Muthgasse 18, A-1190 Vienna, Austria. https://orcid.org/0000-0003-2668-1265 (F. Benedetti)

feature, an IL15-linker, was incorporated into the molecule (Vallera et al. 2016). Simultaneous targeting of two activating receptors of NK cells, NKp46 and CD16, by trifunctional natural killer (NK) cell engagers (NKCEs), directed against a tumor cell antigen, led to a higher potency *in vitro* than could be observed with clinical antibodies directed against the same target (Gauthier et al. 2019). The complex phenomenon of NK-cell engagement appears as a mechanism where trispecific antibodies promise an advantage: intense efforts are invested in NKCEs, directed at the multiple myeloma antigens B-cell maturation antigen (BCMA) and CD200 (Gantke et al. 2017). In another prominent example, an anti-CD38/CD3/CD28 antibody was able to potentiate the killing of CD38-positive myeloma cells by CD3-engagement on cytotoxic T cells by simultaneously engaging the co-stimulatory molecule CD28 on T cells, thus preventing their anergy (Wu et al. 2020).

Molecular design of trispecific antibodies embodied the lessons learned from the plethora of formats of bispecific antibodies: the versatility in valency of antigen engagement, fine tuning of the affinity of a particular binding site and even the distance between the antigen binding sites can be adjusted for their optimal biological activity. Conveniently, well-characterized antigen-binding domains of monoclonal antibodies can often be used as building blocks for trispecific antibodies (Wu and Demarest 2019). Importantly, the final format of a trispecific molecule can be chosen at will from several possible constellations, as presented for NKCE variants where an immunoglobulin (Ig)-like format with a fused Fab fragment assigning an additional specificity was shown to possess favorable pharmacokinetic properties (Gauthier et al. 2019). The BCMA/CD200/CD16A specific antibody is a trispecific tetravalent 'aTriFlex' antibody, a fusion protein featuring bivalent engagement of CD16A on the natural killer cells, and enhanced selectivity via the combination of two low-affinity binding single-chain antibodies for BCMA and CD200 (Gantke et al. 2017). In another study, the anti-CD38/CD3/CD28 antibody was designed with an anti-CD38 Fab on one arm and an anti-CD3/anti-CD28 cross-over dual variable (CODV)-Fab (Steinmetz et al. 2016) on the other arm (Wu et al. 2020). A novel, very inventive approach yielded a trispecific '2 + 1' antibody with an additionally fused Fab-arm, where the common light chain strategy was applied to circumvent promiscuous pairing (Bogen et al. 2021). Besides favorable biophysical properties assuring future manufacturability, attention is paid to the positioning of antigen-recognizing units not to cause steric occlusion of the individual binding sites. Among several designs of the bispecific formats available today, Ig-like molecules are particularly popular as they have more predictable biodistribution and pharmacokinetic properties and are generally easier to produce than fusion formats with scFvs, which have an intrinsic tendency to aggregate (Husain and Ellerman 2018).

In this paper, we describe trispecific antibodies constructed by introducing heterologous Fab-arms into a symmetrical bispecific Ig-like molecule. Due to its minimal deviation from an IgG, we have chosen the mAb^2 format which harbors a novel antigen-binding site in the C_H3 domains of the antigen-binding Fc fragment (Fcab), with a small number (typically 8–13) of modified amino acid residues (Wozniak-Knopp et al. 2010). Until now, four molecules from this platform have entered clinical trials (Gaspar et al. 2020; Kraman et al. 2020; Lakins et al. 2020; Leung et al. 2015). To join two different antibody halves, we have used a method that allows asymmetric pairing of two separately produced parental antibodies of the IgG1 class: after the introduction of a single amino acid mutation at the interface of their complementary C_H3 domains, which disturb the natural stabilizing interaction of an aromatic and a charged residue, hybrid Fab-arm exchanged antibodies are obtained using reduction and re-oxidation of hinge cysteines and subsequent purification via ion exchange chromatography (Labrijn et al. 2013, 2014). This elegant method of heterodimerization thus does not imply the question of promiscuous light chain pairing and has proven efficient by delivering several candidate bispecific molecules currently tested in clinical trials (Grugan et al. 2017; Moores et al. 2016). Practicality of this approach was also confirmed by the development of similar platforms using reduction and re-oxidation of separately expressed antibodies by other groups (Strop et al. 2012). The biophysical properties of our novel trispecific molecule with Fabs recognizing the tumor markers epithelial growth factor receptor (EGFR) and Her2, and an Fcab recognizing the angiogenesis-promoting cytokine vascular endothelial growth factor (VEGF) (Wozniak-Knopp et al. 2017), have been improved by the introduction of one or two point mutations per antibody chain (Scheme in Supplementary Figure 1A–C), and its intended composition has been confirmed using mass spectrometry. Its antigen binding properties have been characterized with a cell surface binding assay and biolayer interferometry (BLI). This trispecific molecule was examined for its internalization properties and anti-proliferative effect for an EGFR and Her2 overexpressing cell line. Based on the discovered design principles, a second bispecific molecule with Fab-arms binding to Angiopoietin2 (Ang2) and VEGF (Scheme in Supplementary Figure 1D) was endowed with an Fc fragment with VEGF-inhibitory activity and shown to be more active than the Fab-arm exchanged hybrid of wild-type Fc-antibodies in inhibiting the growth of HUVEC cells.

Results

We attempted to extend the functionality of bispecific antibodies by assigning a different antigen binding site to symmetric bispecific mAb^2 molecules using chemical reduction and re-oxidation. We first examined the consequences of introducing substitutions F405L (mutation A) and K409R (mutation B) (EU numbering) (Edelman et al. 1969) into a wild-type Fc and an anti-VEGF Fcab CT6 (Figure 1A) (point mutations introduced are labeled with capital letters as defined in Figure 1B). This Fcab is modified in the AB, CD and EF loop as well as in the *C*-terminus of the C_H3 domain to mediate binding to VEGF with nanomolar affinity as well as inhibition of its biological activity (Wozniak-Knopp et al. 2017), and can still bind to VEGF with a high affinity when expressed as a heterodimer with one wild-type C_H3 domain (Lobner et al. 2017b). While the elution profile in size exclusion chromatography (SEC) in native conditions of wild-type Fc variants was not altered, CT6_A Fcab eluted at a later time point with a broader elution profile, indicating a stronger interaction with the column matrix, which could result from partial unfolding (Supplementary Figure 2A). The first model Fab-arm exchanged molecule included the Fab sequences of clinically applied antibodies cetuximab (CX) recognizing EGFR and trastuzumab (TRA) recognizing Her2 (all sequences in Supplementary Table 1). Although variants of CX-CT6_A and B, as well as TRA-CT6_A and B all displayed a sharp monomeric SEC profile indistinguishable from the wild-type (Supplementary Figure 2B and 2C), the expression yield of CX-CT6_B was reduced by about 30%, so the variants CX-CT6_A and TRA-CT6_B were chosen to produce first hybrid antibodies and set the base for optimization of their molecular structure.

Next, we attempted to produce Fab-arm exchanged antibodies with CX-A and TRA-B with wild-type C_H3 domains as well as their mAb^2 variants (Figure 1A). The SEC profiles of the bispecific molecules with wild-type Fc were monomeric and sharp (Supplementary Figure 2D), but the elution peak of the mutant with TRA-CT6_B chain appeared broader than the ones characteristic for parental antibodies (Supplementary Figure 2E). The preparation of Fab-arm exchanged antibody with CT6 in both chains without further modifications contained 5% of aggregate (Supplementary Figure 2F). Therefore, a series of point mutations previously reported to increase the stability of

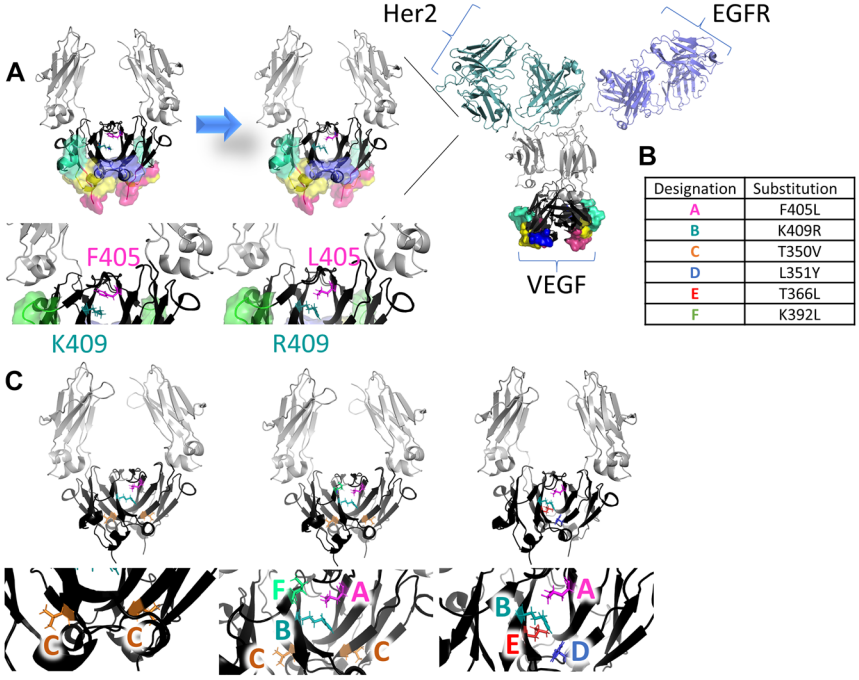

Designation	Substitution
A	F405L
B	K409R
C	T350V
D	L351Y
E	T366L
F	K392L

Figure 1: Molecular design of trispecific mAb^2-based antibodies.
(A) Cartoon model of CT6 Fcab with C_H2 domains in gray and C_H3 domains in black. Mutated residues are surfaced: AB-loop in blue, CD-loop in greencyan, EF-loop in yellow and *C*-terminus in hotpink. Residues F405 (magenta) and K409 (teal) (left panel) are mutated to L and R, respectively (middle panel) to enable the formation of heterodimeric antibody (right panel): CX-Fab in slate blue and TRA-Fab in light teal. Structural files used were PDB: 5K65 for Fcab and PDB: 1HZH for the IgG. The Figure was prepared using PyMOL (Schrödinger, Inc.). (B) Table with designations of tested mutations. (C) Positions of stabilizing point mutations tested in the context of CT6 clone and heterodimeric antibodies. Structural file used was PDB: 5K65. The Figure was prepared using PyMOL (Schrödinger, Inc., New York, USA).

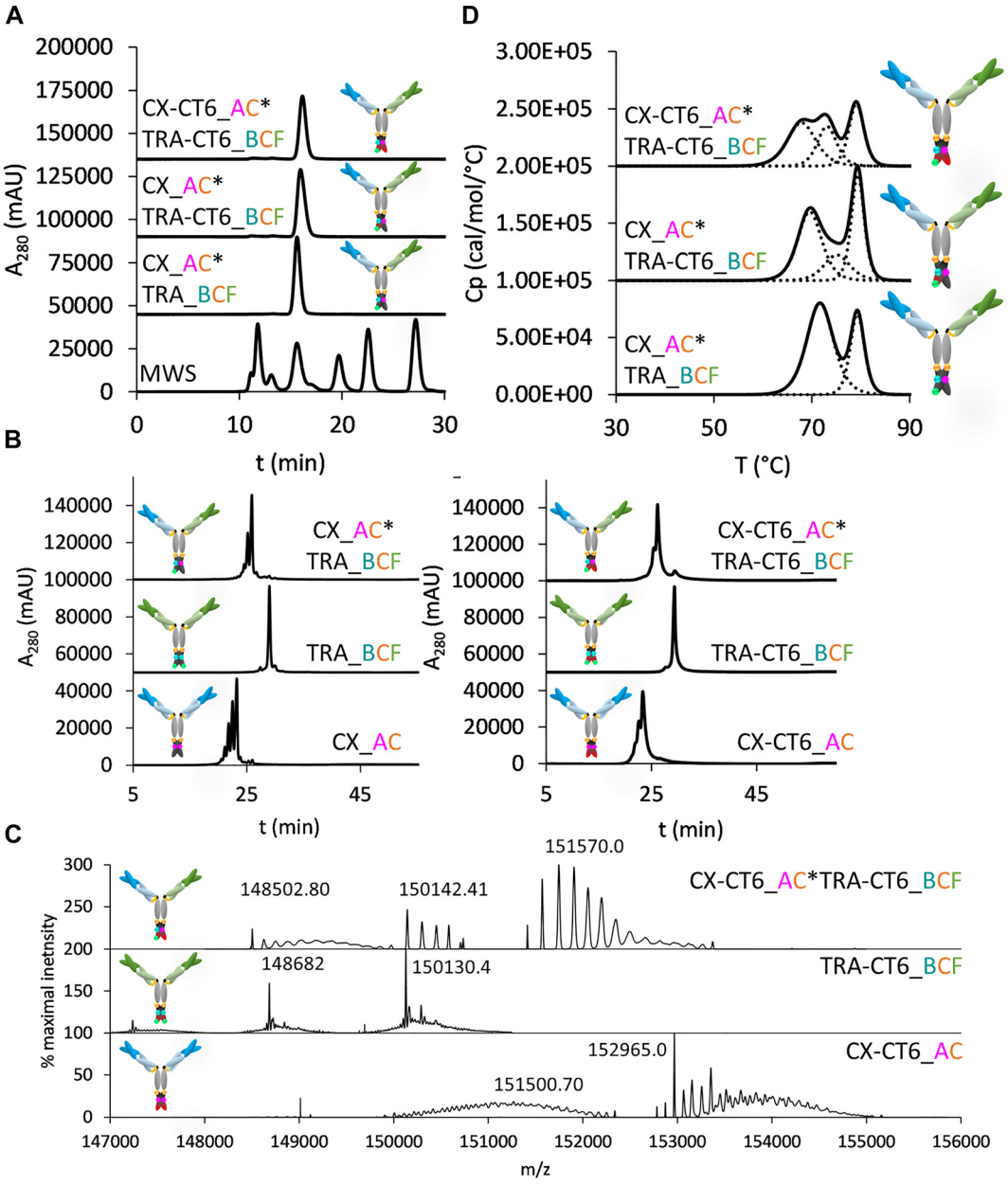

Figure 2: Biophysical properties of controlled Fab-arm exchanged antibodies and their building blocks.
(A) HPLC-SEC profiles of the CX_AC*TRA_BCF with none, one or two CT6-C_H3 domains, chosen for further characterization. MWS (molecular weight standard) contained markers of 670, 158, 44, 17 and 1.35 kDa in size. (B) Ion-exchange chromatography of antibodies with no CT6 (left panel) and with CT6 in both C_H3 domains (right panel). (C) Mass spectrometry analysis of parental antibodies and hybrid antibody CX-CT6_AC*TRA-CT6_BCF. (D) Deconvoluted DSC-profiles of hybrid antibodies CX_AC*TRA_BCF with none, one or two CT6-C_H3 domains.

the heterodimeric antibodies (von Kreudenstein et al. 2013) was tested for their effect on mutated mAb^2 molecules. In particular, mutations T350V (mutation C) on both chains of the antibody, mutation L351Y (mutation D), which exerts its thermostabilizing effect when combined with the T366L (mutation E) of the complementary chain, and K392L (mutation F) were examined (Figure 1C). None had a negative effect on the wild-type versions of the parental antibodies (Supplementary Figure 2G), but the mutation E caused aggregation of TRA-CT6_B (Supplementary Figure 2H), and therefore this variant as well as CX-CT6_AD were not further studied. SEC profiles of wild-type hybrid antibodies with exchanged Fab-arms without further modifications, as well as variants carrying mutation C in both chains, or C in both

Table 1: Results of mass spectrometry analysis of Fab-arm exchanged CX-CT6_AC*TRA-CT6_BCF and the parental antibodies.

	Theoretical mass	Observed mass	Difference in mass	Glycosylation	Mass error
			(Da)		
Parental antibodies					
CX-CT6_AC	147,195.6	152,965.0	5769.4	4xG0F	−11
TRA-CT6_BCF	147,233.8	150,130.4	2896.6	2xG0F	+6
Fab-arm exchanged antibody					
CX-CT6_AC*TRA-CT6_BCF	147,214.6	151,570.0	4355.4	3xG0F	+20

G0F glycan: asialo-agalacto-fucosylated biantennary oligosaccharide.

and F in TRA_B chain, were indistinguishable from parental mAb^2 molecules in SEC-HPLC (Figure 2A and Supplementary Figure 2D–F).

When combining complementary antibody chains, the hybrid antibody CX_AC*TRA-CT6_BCF eluted as a sharp peak (Figure 2A), unlike when only mutation C was present in both chains (Supplementary Figure 2E). Importantly, SEC-HPLC profiles of all stabilized variants of Fab-arm exchanged antibodies with CT6 in both chains were monomeric and sharp (Supplementary Figure 2F). Nevertheless, we decided to characterize also the variant with analogous mutations as present in the best hybrid antibody with a single VEGF-binding C_H3 domain.

The initial information on the composition of the Fab-arm exchanged antibody was obtained using ion-exchange chromatography, where we could distinguish the hybrid variant from both parental antibodies (Figure 2B). Correct pairing of the heterodimeric antibodies was examined using mass spectrometry of the intact antibodies. The Fab-arm exchanged trispecific antibody was proven to be composed of the halves of parental antibodies, with only small differences from the calculated molecular weight (Figure 2C and Table 1), where the values of −11 Da results most likely from *N*-terminal glutamate to pyroglutamate conversion and +20 Da from oxidation.

Importantly, the overall thermostability of the Fab-arm exchanged antibodies was high (Figure 2D, Supplementary Figure 3 and Supplementary Table 2). For the variants without CT6-modifications two midpoints of thermal transitions at about 71 and 79 °C could be observed, corresponding to denaturation of CX-Fab and the C_H2 domains (T_M1), and denaturation of TRA-Fab and C_H3 domains (T_M3). In the Fab-arm exchanged antibodies with CT6, another transition (T_M2) was recorded at about 73 °C, corresponding to thermal denaturation of the C_H3 domain of the CT6 clone, which agrees with published data (Wozniak-Knopp et al. 2017). The actual positive shift in thermostability of the chosen combinations of mutations was not large, with maximal 1.3 °C for T_M1, 2.1 °C for T_M2 and 0.5 °C for T_M3 for the mutants with CT6 on TRA-chain (Supplementary Figure 3 and Supplementary Table 2).

Next, we tested functional bispecific binding of the Fab-arm exchanged trispecific antibodies. Strongly EGFR-positive and Her2-negative cell line MB-MDA-468 was incubated with serial dilutions of Fab-arm exchanged antibodies with one or two VEGF-binding C_H3 domains, and the binding was detected once with an anti-kappa chain conjugate to examine the activity of CX-derived Fab-arm, and once with biotinylated VEGF addressing the simultaneous binding via CT6. In the constructs, composed of the CX-chain with a wild-type C_H3 domain, combined with the TRA-chain with the CT6 domain, binding can only occur if the Fab-arm exchange has taken place. All tested proteins were similar in cell binding with an EC_{50} of about 4 nM, and strong simultaneous binding to EGFR and VEGF was detected with all Fab-arm exchanged antibody variants (Figure 3A). The proteins with a single VEGF-binding C_H3 domain displayed a lower plateau of fluorescence upon saturation, which results likely from loss of avid binding; a heterodimer with a wild-type C_H3 and a CT6-C_H3 was previously characterized with a dissociation constant (K_D) of 18 versus 4 nM, determined for homodimeric CT6, for solution binding (Lobner et al. 2017b). Quantitative evaluation by biolayer interferometry (BLI) of VEGF-binding parameters has shown that the Fab-arm exchanged antibodies with two CT6-domains bind with an affinity equal to parental mAb^2 molecules, indicating that antigen binding properties of the Fcab are preserved in the novel multispecific format (Figure 3B and Supplementary Table 3). Indeed, the tested trispecific antibody could be immobilized on VEGF-coated sensors and still interact with other two cognate antigens, EGFR and Her2 (Figure 3C).

We then compared the anti-proliferative activity of EGFR/Her2/VEGF trispecific molecule on an EGFR/Her2 overexpressing cell line A431, which expresses 2.1×10^6 EGFR and 1.5×10^5 Her2 receptors per cell (Björkelund et al.

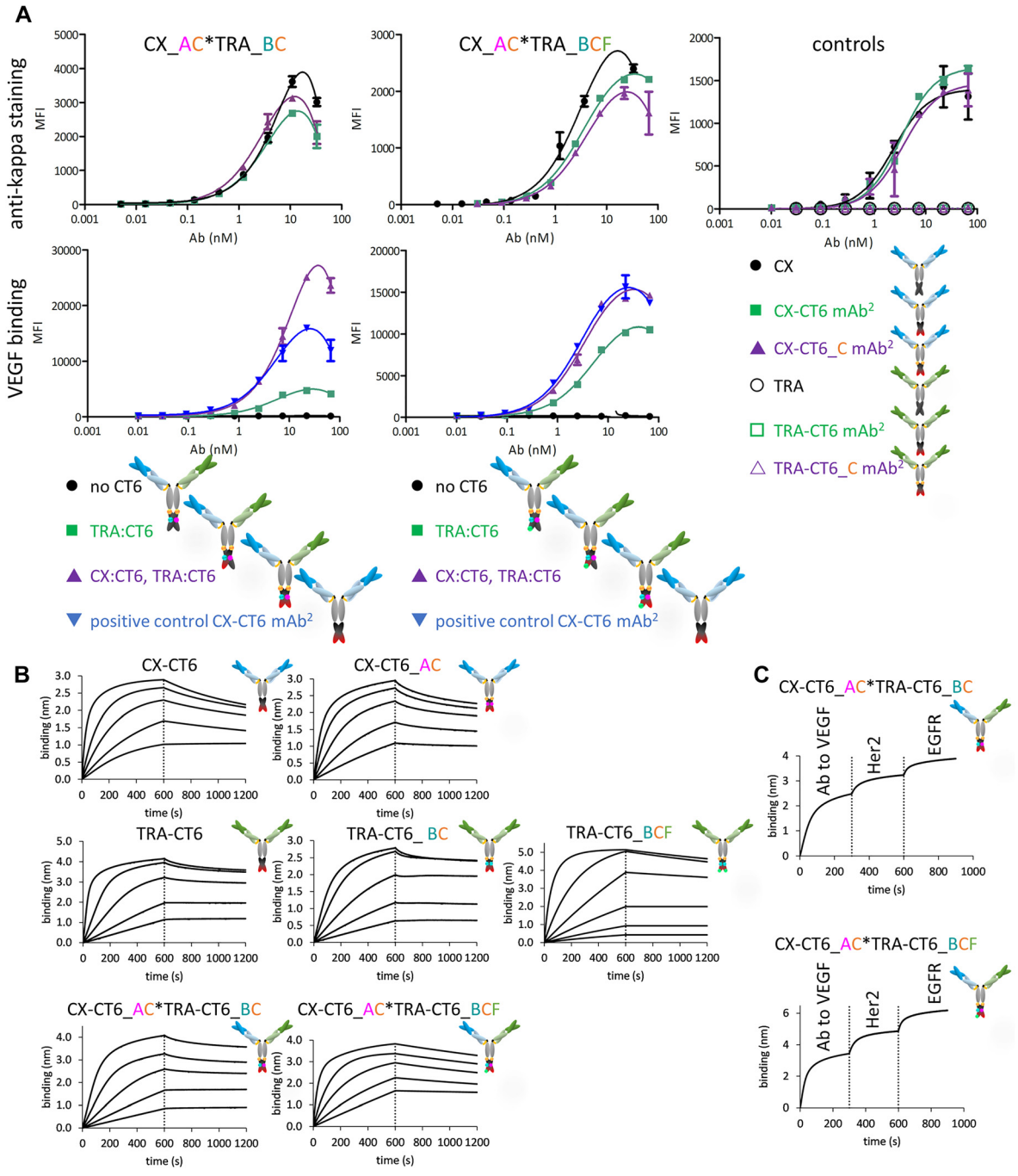

Figure 3: Antigen-binding properties of hybrid antibodies.
(A) Binding to the surface of EGFR-positive cells, detected with an anti-kappa conjugate (upper panels) or biotinylated VEGF (lower panels), for CX_AC*TRA_BC variants (left panels) and CX_AC*TRA_BCF variants (middle panels) with CX- or TRA-arms only controls (right panels). (B) Results of biolayer interferometry (BLI) experiment measuring binding to VEGF for CX-based mAb^2 and CX mAb^2-building block (upper panels), TRA-based mAb^2 and TRA mAb^2-building blocks (middle panels) and Fab-arm exchanged antibodies (lower panels). (C) BLI experiment to observe binding of the Fab-arm exchanged antibodies to VEGF, and their sequential association to Her2 and EGFR.

2011) with the effect of parental mAb^2 molecules and the bispecific anti-EGFR/Her2 construct. Parental mAb^2 CX-CT6 could significantly reduce the proliferation with or without the addition of 200 nM VEGF, and also the parental mAb^2 TRA-CT6 and Fab-arm exchanged bispecific antibody were anti-proliferative without addition of VEGF (Figure 4A). The anti-proliferative effect of trispecific antibody was significant even without VEGF addition, however with VEGF a

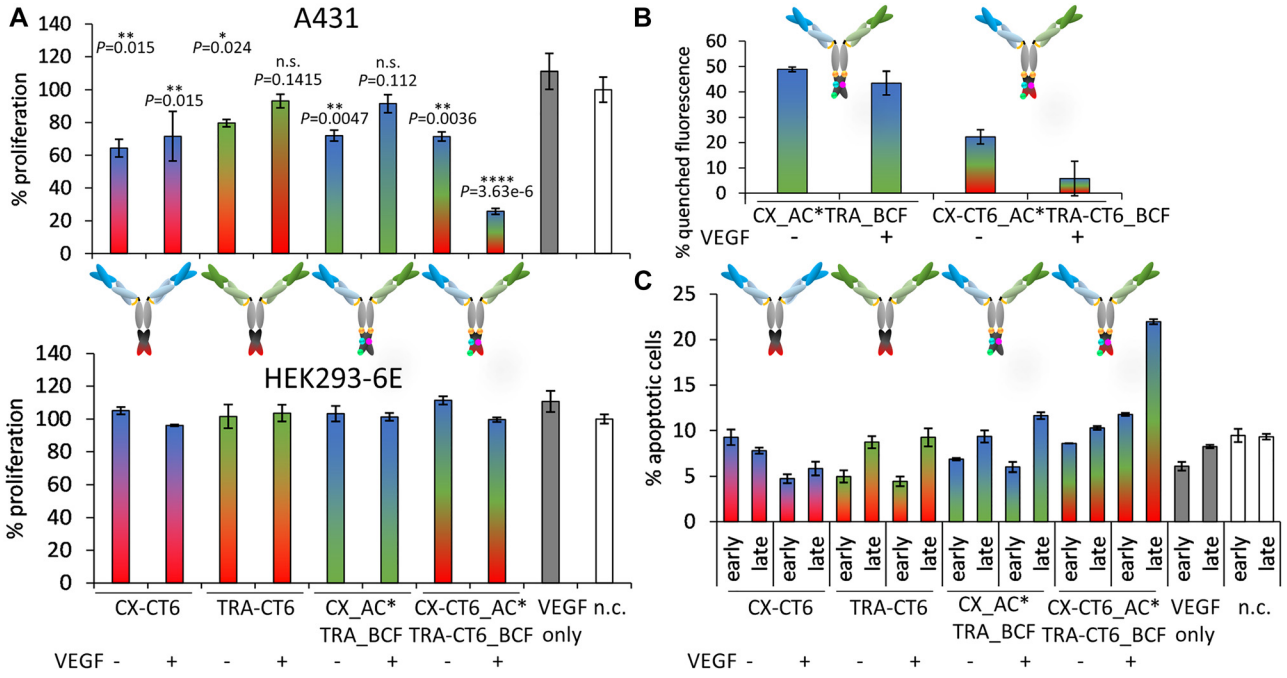

Figure 4: Biological effect on anti-EGFR/Her2/VEGF antibody on EGFR/Her2 overexpressing A431 cell line.
(A) Proliferation of A431 cells (upper panel). Effects of antibodies were compared with cells with VEGF only or non-treated controls (n.c.), respectively. Sample size was $n = 6$ for antibody treatments and $n = 9$ for VEGF-only and n.c. One-way ANOVA was used to determine the significance (n.s. [not significant] $0.05 \le P$, $*0.01 \le P < 0.05$, $**0.001 \le P < 0.01$, $***0.0001 \le P < 0.001$, $****P \le 0.0001$) in comparison with VEGF-only or untreated cells, respectively. Control HEK293-6E cells were not affected by the treatment (lower panel). (B) Internalization of Fab-arm exchanged bispecific and trispecific antibody into A431 cells with or without VEGF addition ($n = 2$, error bars represent SD). (C) Percentage of early (annexinV-positive-PI negative) and late (annexinV-positive-PI positive) apoptotic A431 cells after 5 days of treatment with antibodies. ($n = 2$, error bars represent SD).

significantly stronger effect was observed ($P < 0.05$) than with any of the control proteins (Figure 4A, upper panel), which was specific to antigen-expressing cells as the control cell line HEK293-6E remained unaffected (Figure 4A, lower panel). Internalization of the trispecific construct proceed rapidly with less than 5% detectable on the cell surface after an overnight incubation when cross-linked with VEGF and 25% without cross-linking, in comparison with about 50% of bispecific Fab-arm exchanged antibody regardless of VEGF addition (Figure 4B). As higher levels of annexinV-positive cells were detected in cultures treated with VEGF-crosslinked CX_AC*TRA_BCF in comparison with those treated with parental mAb^2 molecules and bispecific Fab arm-exchanged antibodies (Figure 4C), induction of apoptosis can be considered the main mechanism of action of the trispecific antibody.

As the antibody-dependent cytotoxicity (ADCC) is an important mode of action of parental antibodies, we also inquired the ADCC potency of the trispecific antibody on the EGFR-overexpressing cells MB-MDA-468 in a T-cell reporter assay. Trispecific CX_AC*TRA_BCF antibody and bispecific CX_AC*TRA_BCF antibody activated the engineered cells with an EC_{50} of about 2.5 nM, which was about five-fold higher than the EC_{50} determined for CX and CX-CT6 mAb^2 (Supplementary Figure 4).

We further tried to use Fab-arm exchange to engineer an additional antigen binding site into a bispecific antibody with different Fab sequences. Bevacizumab (BEV) is a clinically broadly used anti-VEGF antibody (Garcia et al. 2020), whose inhibitory effect on growth of HUVEC cells *in vitro* could be potentiated by incorporating CT6 Fcab into its constant domains (Wozniak-Knopp et al. 2017). The other Fab-arm in this construct, derived from Ang2 mAb C49T (ANG) (Buchanan et al. 2013), binds to Ang2, a key regulator of tumor angiogenesis and blood vessel remodeling. Simultaneous blocking of Ang2-mediated signaling and VEGF-induced blood vessel growth has already proven a therapeutically efficient mechanism, powered for example by Faricimab, a bispecific monoclonal antibody designed for intravitreal use and currently in advanced clinical studies of neovascular age-related macular degeneration and diabetic macular edema (Nicolò et al. 2021). Parental antibodies ANG and BEV with mutations A and B were alike the wild-type molecules in HPLC-SEC in native conditions, but ANG-CT6_A displayed strong aggregation (Supplementary Figure 5). Introduction

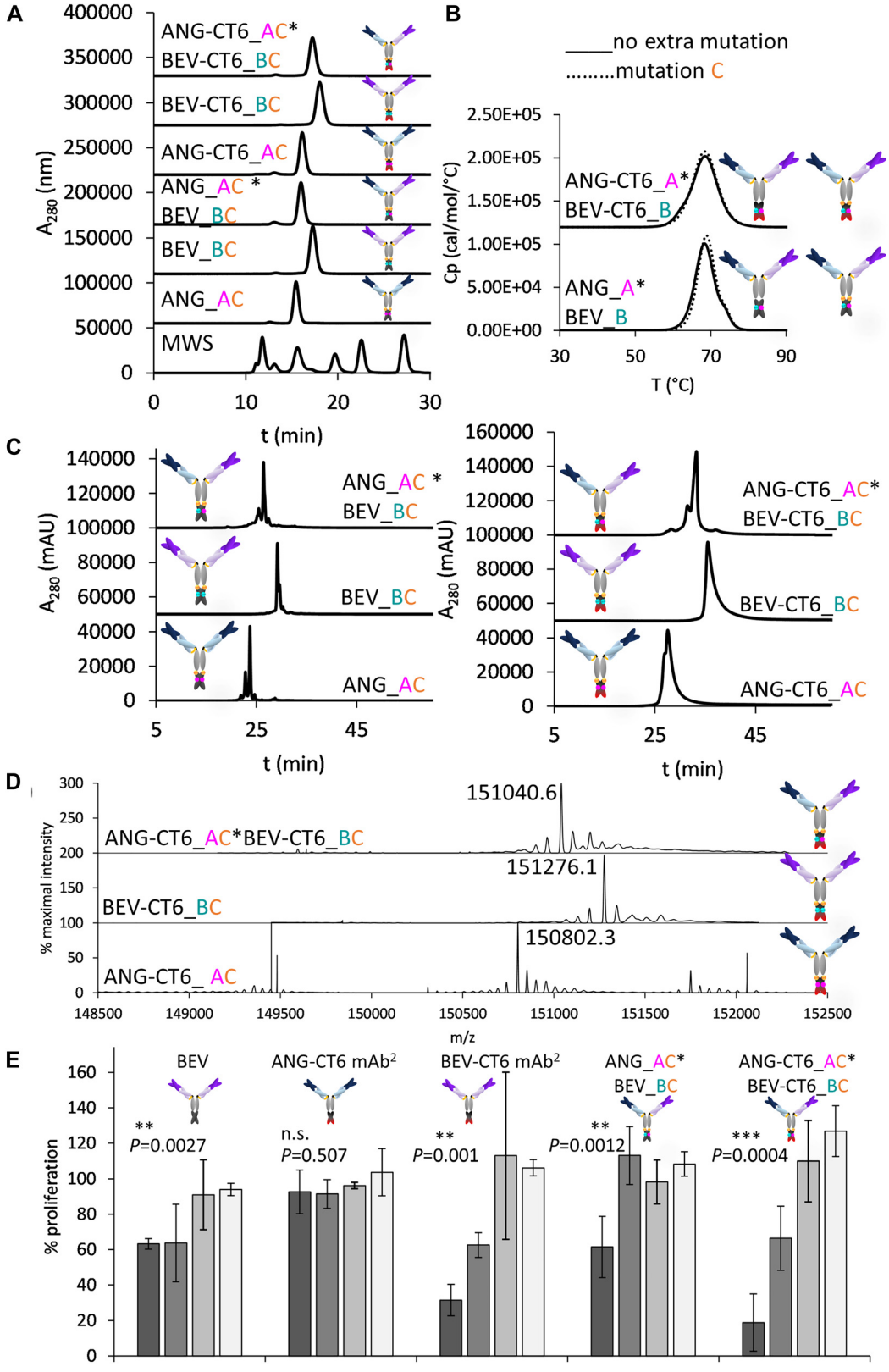

Figure 5: Characterization of ANG*BEV-based Fab-arm exchanged antibodies.
(A) HPLC-SEC of mutation C-endowed variants of the building blocks and Fab-arm exchanged antibodies with no and 2 CT6-C_H3 domains. MWS (molecular weight standard) contained markers of 670, 158, 44, 17 and 1.35 kDa in size. (B) DSC analysis of mutation C-endowed and wild-type

of mutation C rendered the HPLC-SEC profile of this construct wild-type like (Figure 5A). Upon the introduction of this mutation in both antibody chains the positive effect on thermostability amounted to about 2 °C positive shift from the wild-type (Figure 5B). Fab-arm exchanged antibodies were distinguished from the parental molecules with ion-exchange chromatography (Figure 5C), and mass spectrometry analysis confirmed the formation of the expected heterodimer (Figure 5D and Table 2). We could also detect a good affinity towards the antigens Ang2 and VEGF in ELISA (Supplementary Figure 6A and 6B). The trispecific heterodimer was tested for its ability of inhibition of HUVEC cell proliferation and reduced their proliferation down to 18% at 5.76 nM (Figure 5E). At this concentration, the antiproliferative effect of BEV, BEV-CT6 and the bispecific Fab-arm exchanged antibody was also significant (Figure 5E), but trispecific antibody was more potent than BEV alone ($P = 0.035$) and ANG*BEV Fab-arm exchanged bispecific antibody ($P = 0.0363$), and similar as the parental BEV-CT6 mAb^2. ANG-CT6 mAb^2 was not active in the assay at this concentration, as only the effect of VEGF inhibition is measured and the activity of the anti-VEGF Fcab alone is expected to be detected at about 50 nM (Wozniak-Knopp et al. 2017). The release of Ang2 from endothelial cells is dependent on stimulus, such as wound healing or tumor growth and only then Ang2-blockers can be applied to limit tumor extravasation (Khan et al. 2021).

Discussion

Trispecific antibodies are considered very promising targeting agents, as the incorporation of an additional specificity expands the repertoire of addressed molecules and includes freedom in design of the multiplicity of specificities and antigen binding valency. This can be of advantage, when cells with defined complex patterns of surface molecules should be specifically recognized for the purpose of higher selectivity and hence superior safety, such as mediated by several low-affinity binders that will only form a stable interaction when multiple targets are present (Sellmann et al. 2016). Especially in immunooncology such agents can trigger a precise combination of signals that has to be delivered to molecular switches acting in various modes (Garfall and June 2019), and extend the reach of present therapeutic options to prove functional in biological situations that are currently considered difficult to address. The promise of trispecific targeting agents goes beyond their envisioned application in soluble format: trispecific CAR-T cells simultaneously targeting three B cell leukemia antigens (CD19, CD20, and CD22) proved superior to monospecific CAR-T cells in mouse models (Schneider et al. 2017), and such therapies could prevent the disease relapse due to antigen loss or the down-regulation of target antigen in B cell malignancies.

Here we have established a novel method of applying a controlled Fab-arm exchange mechanism to preexisting bispecific antibodies. Using two different combinations of parental antibodies, we could produce asymmetrical antibodies with an additional antigen binding site located in the C_H3 domains. Resulting trispecific tetravalent molecules show correct chain composition. Although in the chosen Fcab clone 22 amino acid residues have been modified to achieve high-affinity antigen binding, one or two stabilizing point mutations were sufficient to produce desired Fab-arm exchanged antibodies with favorable biophysical properties. Interestingly, the mutation C, beneficial for their SEC-HPLC profile, was previously reported to have only a negligible positive effect on thermostability in C_H3:C_H3 domain complex (Dall'Acqua et al. 1998; von Kreudenstein et al. 2013). The relatively small number of amino acid substitutions applied, all of which are located in the interface of the C_H3:C_H3 domains shielded from solvent, also reduces the risk of immunogenicity (Ulitzka et al. 2020). Importantly, antigen affinity and biological activity of the Fcab part was not affected by the reduction and re-oxidation procedure required for the controlled Fab-arm exchange. The interesting finding that the anti-EGFR/Her2/VEGF antibody can induce apoptosis of cells overexpressing both receptors underlines the possibility of exciting novel biology that can be discovered for multispecific molecules. The potent effect was induced upon addition of VEGF and increased concentrations of VEGF are typical for tumors of various types (Kut et al. 2007). It is likely that in our experiments some cross-linking occurred also without the VEGF addition via the VEGF secreted by A431 cells (0.08 pg/ml per cell per day) (Hamma-Kourbali et al. 2003). Potent VEGF blocking by ANG*BEV-CT6 also promises extended

variants of the Fab-arm exchanged antibodies with none and 2 CT6-C_H3 domains. (C) Ion-exchange chromatography of antibodies with no CT6 (left panel) and with CT6 in both C_H3 domains (right panel). (D) Mass spectrometry analysis of parental antibodies and hybrid antibody ANG-CT6_AC*BEV-CT6_BC. € Activity of Fab-arm exchanged antibodies in HUVEC proliferation assay (bars present the 5.76, 0.576, 0.0576, and 0.00,576 nM concentration) for $n = 3$ for incubation with BEV, ANG-CT6 and BEV-CT6 mAb^2 and $n = 4$ for the incubation with Fab-arm exchanged antibodies (error bars represent SD). One-way ANOVA was used to determine the significance at 5.76 nM concentration (n.s. [not significant] $0.05 \le P$, *$0.01 \le P < 0.05$, **$0.001 \le P < 0.01$, ***$0.0001 \le P < 0.001$, ****$P \le 0.0001$) in comparison with untreated cells.

Table 2: Results of mass spectrometry analysis of Fab-arm exchanged ANG-CT6_AC*BEV-CT6_BC and the parental antibodies.

	Theoretical mass	Observed mass	Difference in mass	Glycosylation	Mass error
			(Da)		
Parental antibodies					
ANG-CT6_AC	147,930.6	150,802.3	2871.1	2xG0F	−19
BEV-CT6_BC	148,374.7	151,276.1	2901.4	2xG0F	+1
Fab-arm exchanged antibody					
ANG-CT6_AC*BEV-CT6_BC	148,157.6	151,040.6	2882.9	2xG0F	−7

G0F glycan: asialo-agalacto-fucosylated biantennary oligosaccharide.

functionality in comparison with bispecific Fab-arm exchanged antibody.

We observed that the ADCC potency of our bispecific and trispecific Fab-arm exchanged constructs based on CX and TRA is lower than for wild-type CX and CX-CT6 mAb^2, but the potent antiproliferative effect of the trispecific antibody was induced by internalization and apoptosis and did not require effector cells. An important difference from CX and CX-CT6 in the ADCC assay is the monovalent antigen engagement by the Fab-arm exchanged constructs, however it has already been noted that the reactivity of Fab-arm exchanged constructs with FcγRIIIa, the ligand molecule for ADCC-mediating effector cells, can be lower than for parental antibodies (Grugan et al. 2017) and their defucosylation can improve their ADCC potency, as for example in clinically approved anti-EGFR/met antibody amivantamab (Neijssen et al. 2021).

In course of optimization of the trispecific molecule, we have utilized a construct with one wild-type and one VEGF-binding C_H3 domain to enable a quick estimation of binding functionality of novel hybrid antibodies. Surprisingly, the SEC-HPLC profile of this molecule was broader than observed for antibodies with two antigen-binding C_H3 domains. This could be a result of incompatibility of both C_H3 interfaces, resulting in their less stable interaction and temporary exposure of the interface ('breathing'). On the other hand, mutated residues in CT6 clone form a network of aromatic rings which contribute to π-π stacking and enhanced stability (Lobner et al. 2017b).

In most described cases, antigen engagement by Fcabs is bivalent (Lobner et al. 2017a,b). Besides producing antibodies with more than two specificities, Fab-arm exchanged antibodies with Fcabs offer the possibility of monovalent antigen engagement, which can be advantageous in certain biological settings, for example to avoid undesired cross-linking of the receptors, as in case of c-met, causing agonism (Pacchiana et al. 2010), or achieve superior safety, such as in case of CD3-targeting agents, where the likelihood of inducing 'cytokine release syndrome' can be minimized (Wang et al. 2021). It will be also interesting to explore to what extent different half-Fcabs, featuring diverse degrees of deviations from the wild-type Fc in the extent of mutagenesis, can be combined even to tetraspecific molecules.

Materials and methods

Molecular design

Constructs for heavy and light chains were cloned in pTT vectors (Canadian National Research Council [CNRC], Ottawa, Ontario, Canada). Mutagenesis of the positions in the complementary C_H3 domains that allow later chemical reduction and heterodimerization per oxidation (A and B) was performed using Quikchange Lightning mutagenesis kit (Agilent, Santa Clara, California, United States) using oligonucleotides listed in Supplementary Table 4, exactly according to manufacturer's instructions. A series of point mutations, described to assign a thermostabilizing effect on heterodimerized complementary C_H3 domains, was introduced using the same method (sequences of oligonucleotides in Supplementary Table 4 and structural models in Figure 1). Nucleotide sequences of all constructs were verified using Sanger sequencing.

Protein production and purification

HEK293-6E cells (CNRC) were cultured in F17 medium (Thermo Fisher Scientific, Waltham, Massachusetts, United States) supplemented with 4 mM L-glutamine, 1% Pluronic P-68 (Thermo Fisher Scientific) and 0.25 mg/ml G-418 antibiotic at 37 °C, in humidified atmosphere with 5% CO_2 on an orbital shaking platform at 125 revolutions per min (rpm). Plasmid DNA with heavy and light chain in a 1:1 mass ratio was transfected together with double mass of polyethyleneimine, 1 µg DNA per ml cells at a density of 1.7–2.0 × 10^6/ml. Two days post transfection, cells were fed 0.25% TN-1 tryptone and the expression continued for further three days. Supernatants were harvested with centrifugation at 2300 *g* for 20 min at 4 °C, buffered to 0.1 M Na-phosphate buffer, pH 7.0, and clarified using filtration through a 0.45 µm filter (Merck Millipore, Burlington, Massachusetts, United States). After loading onto a 1 ml-Protein A HP column (Cytiva, Marlborough, Massachusetts, United States) at 1 ml/min, unbound material was washed with 0.1 M Na-phosphate buffer, and antibodies were eluted with 0.1 M glycine, pH 3.5 and neutralized immediately with the addition of 2 M Tris base. The dialysis against at least 100-fold volume

of PBS (Thermo Fisher Scientific) proceeded in Snakeskin dialysis tubing with 10,000 Da molecular weight cut-off (MWCO) (Thermo Fisher Scientific) overnight at 4 °C with constant stirring. Concentration of the antibodies was determined by measuring A_{280nm} with a NanoDrop Spectrophotometer (Thermo Fisher Scientific). Antibody preparations were stored at −80 °C until further use.

Preparation of hybrid antibodies

Complementary antibodies at a concentration of 1 mg/ml were treated with 50 mM 2-mercapoethanolamine (2-MEA) overnight at room temperature (RT) with gentle agitation. Preparations were mixed in an equal ratio and the buffer was exchanged to PBS using ZebaSpin columns with 40,000 Da MWCO (Thermo Fisher Scientific) exactly according to manufacturer's instructions. Preparations were stored at −80 °C until further use.

Chromatographic methods

Size exclusion chromatography (SEC): SEC-high performance liquid chromatography (HPLC) was performed with a Superdex 200 Increase 10/300 GL column (Cytiva) running on a Shimadzu LC-20A Prominence system (Shimadzu, Kyoto, Japan) equipped with a diode array detector. Chromatography was conducted with a constant flow rate of 0.75 ml/min with PBS with 200 mM NaCl as the mobile phase buffer used. A total of 20 µg protein at about 1 mg/ml was loaded on the column for analysis. Column calibration was performed with a set of molecular mass standards ranging from 1.3 to 670 kDa (Bio-Rad, Hercules, California, United States).

Ion exchange chromatography (IEX): For IEX-HPLC, 50 µg of the antibody was applied to a ProPax WCX-10 LC Column (4 × 250 mm) (Thermo Fisher Scientific) equipped with a ProPax WCX-10 LC Guard Column (4 × 50 mm) (Thermo Fisher Scientific), equilibrated with 20 mM MES, pH 6.0 (buffer A) with 3% buffer B (20 mM MES with 750 mM NaCl). For elution the following sequence of steps was applied: 3% buffer B for 5 min, linear gradient from 3–14.6% B in 25 min, linear gradient from 14.6–33.3% B in 30 min, 33.3–100% B in 0.1 min and finally 100% B for 10 min at a flow rate of 1 ml/min.

Differential scanning calorimetry (DSC) analysis

About 5 µM protein solution, diluted in PBS at pH 7.0, was used for thermostability analysis. Heating was performed with Automated MicroCal PEAQ-DSC system (Malvern Panalytical, Malvern, United Kingdom) in the range of 20–100 °C at a rate of 1 °C/min, with repeated scans run at the same conditions to obtain the baselines for subtraction from the first scan. Data was fitted with Origin 7.0 for DSC software and the non-two-state transition mechanism was applied for scan deconvolution and determination of midpoint temperatures of transitions (T_Ms).

Mass spectrometry

To determine the correct pairing of the heterodimer chains, 1 µg of the protein was injected directly to a liquid chromatography-electrospray ionization-mass spectrometry (LC-ESI-MS) system (Dionex UltiMate 3000 Nano HPLC, Dionex Corporation, Sunnyvale, California). A gradient from buffer A (0.1% formic acid) to buffer B (80% acetonitrile [ACN], 0.08% formic acid) was run to reach 12–73% ACN using applying 15% B for 3 min, reaching 50% B in 5 min, 80% B in 1 min and 90% B in 4 min, to an Aeris™ 3.6 µm WIDEPORE C4 200 Å, LC Column 150 × 2.1 mm at a flow rate of 250 µl/min at 50 °C. Detection was performed with a Synapt G2Si instrument (Waters, Milford, Massachusetts, United States) in sensitivity mode. Instrument calibration was performed using ESI calibration mixture (Agilent). Spectrum deconvolution was performed using MaxEnt algorithm.

Biolayer interferometry

Affinity to VEGF: $VEGF_{109}$ isomer with N75Q mutation obliterating an *N*-linked glycosylation site was produced in HEK293-6E cells, purified using Ni-NTA chromatography as described before (Benedetti et al. 2021) and labeled with NHS-LC-LC-biotin (Thermo Fisher Scientific) at a molar ratio of 1:1.5 (protein dimer to biotin) for 2 h at 25 °C. Excess reagent was removed with dialysis against 100-fold volume of PBS (Thermo Fisher Scientific) overnight at 4 °C using Snakeskin dialysis tubing with MWCO of 10,000 Da (Thermo Fisher Scientific). An Octet 96RED (ForteBio)-based assay was used for determination of binding kinetics, using PBS supplemented with Kinetics Buffer (ForteBio, Molecular Devices, Fremont, California, United States) as the assay buffer at 25 °C with the plate shaking at 1000 rpm. Biotinylated VEGF was immobilized on high-precision streptavidin tips (ForteBio) equilibrated in assay buffer at 5 µg/ml for 10 min. Antibody preparations in two-fold dilution series starting at 100 nM were allowed to bind to the immobilized VEGF for 600 s at 25 °C. Dissociation was recorded for 600 s after transfer of the tips into assay buffer. Assay background was determined with a VEGF-coated tip immersed in assay buffer only. After background measurement subtraction, data were fitted with the 1:1 binding model (ForteBio Evaluation Software, version 13.0) as this is the proposed stoichiometry of the interaction of CT6 Fcab with the dimeric VEGF (Lobner et al. 2017b).

Simultaneous antigen binding: To demonstrate the ability of trispecific antibody binding to all three antigens, the assay was performed as above, but after binding of the antibody to VEGF the test sensor was immersed in a 100 nM solution of extracellular domain of Her2-Fc (Sino Biological, Beijing, China) for 300 s, and then in a 100 nM solution of extracellular domain of EGFR-Fc (Sino Biological) for another 300 s. The signal from the VEGF-coated tip with bound antibody, dissociating into assay buffer, was subtracted as background.

ELISA to Ang2 and VEGF

ELISA Maxisorp plates (NUNC, Roskilde, Denmark) were coated with 1 µg/ml Ang2 (Sino Biological) in PBS for 1 h at RT and blocked with 4% bovine serum albumin (BSA) in PBS for 1 h at RT with continuous shaking. The plates were washed three times with PBS prior to the addition of antibodies in three-fold dilutions in 2% BSA starting from 66.6 nM. After 1 h incubation, plates were washed three times with PBS, and 100 µl of anti-human kappa-HRP conjugate (A-7164, Sigma-Aldrich, *Merck* KGaA, Darmstadt, Germany), diluted 1:5000 in 2% BSA-PBS was delivered to each well and incubated for 30 min. The wells were washed three times with PBS, and 100 µl of the developing solution 3,3′, 5,5′-tetramethylbenzidine (TMB) (Sigma-Aldrich) was

added. The reaction was stopped with 100 µl 30% H_2SO_4 and the $A_{450/620nm}$ was measured with a Tecan Sunrise microplate reader (Tecan, Männedorf, Switzerland). Binding to VEGF in this format was tested with a similar protocol except for antigen $VEGF_{109}$N75Q concentration, which was 5 µg/ml, and dilutions of tested antibodies started at 10 µl nM.

Cell culture and tests

Cell culture

EGFR-positive cell lines MDA-MB-468 (ATCC® HTB-132™) (ATCC, Manassas, Virginia, United States), with 1.8×10^6 EGFR molecules per cell (Sellmann et al. 2016) and devoid of Her2, EGFR/Her2 positive A431 cells (ATCC® CRL-1555™) (2.1×10^6 EGFR and 1.5×10^5 Her2 receptors per cell) (Björkelund et al. 2011) and the control cell line HEK293-6E (CNRC) were propagated in Dulbecco's Modified Eagle Medium (DMEM) with 100 U/ml penicillin and 10 µg/ml streptomycin (all Thermo Fisher Scientific) and 10% fetal bovine serum (FBS) (Sigma-Aldrich) at 37 °C in humidified atmosphere under 5% CO_2 and passaged using 0.05% trypsin-0.1% EDTA solution (Sigma-Aldrich) twice a week.

Cell staining

Test cells were harvested from T75 flasks by removing culture medium, rinsing three times with 12 ml PBS, and incubating with 3 ml of trypsin-EDTA solution at 37 °C for 5 min. Nine ml of DMEM with 10% FBS and antibiotics were used to block protease activity. After centrifugation at 300 *g*, 5 min at 4 °C, cells were resuspended in 2% BSA-PBS at a density of 1×10^6/ml and incubated for 30 min on ice. Aliquots of 100,000 cells were distributed into 96-well-U-shaped plates and incubated with graded concentrations of test antibodies in three-fold dilutions starting from 66 nM, diluted in 2% BSA-PBS, for 30 min on ice. Cells were collected at 300 *g*, 5 min at 4 °C, resuspended in 100 µl of anti-human-kappa-$(Fab)_2$′ conjugated with fluorescein-isothiocyanate (FITC) (F-3761, Sigma-Aldrich), diluted at 1:100 in 2% BSA-PBS, and incubated for 30 min on ice. To demonstrate bispecific binding of Fab-arm exchanged antibodies, cells were coated with antibody samples as described above, and then resuspended in 100 µl of biotinylated VEGF at 5 µg/ml in 2% BSA-PBS and incubated for 30 min on ice. Cells were pelleted at 300 *g* for 5 min at 4 °C, supernatant removed and replaced for 100 µl streptavidin-Alexa Fluor 647 (Thermo Fisher Scientific), diluted to 0.5 µg/ml in 2% BSA-PBS. After an incubation for 30 min on ice and a final centrifugation at 300 *g* for 5 min at 4 °C, the cells were resuspended in 200 µl of ice-cold PBS and analyzed using Guava®easyCyte™ flow-cytometry instrument (Luminex, Austin, Texas, United States). Duplicate measurements were performed and EC_{50} was calculated using Prism 5.0, mean and S.E.M. are presented.

A431 proliferation assay

A431 and control HEK293-6E cells were seeded at 10,000 cells per well into 60 inner wells of a 96-F-shaped-well plate (Nunc) in 100 µl DMEM with 10% FBS and antibiotics, sealed with a Breathe-Easy® semi-permeable membrane (Sigma-Aldrich) and incubated overnight at 37 °C. Antibodies were added in the same medium at 66.6 nM in 100 µl-volume per well, with or without 200 nM $VEGF_{109}$ N75Q. Treatment proceeded for 9 days and then medium was replaced with 100 µl of WST-1 reagent (Roche, Basel, Switzerland), diluted 1:10 in DMEM with 10% FBS with antibiotics. The absorbance at 450/620 nm was read out after 2–4 h of incubation at 37 °C under humidified atmosphere with 5% CO_2. Background recorded from the wells without cells was subtracted and readings of wells with cells cultured in medium without added antibodies and VEGF were considered non-treated controls. For A431 cell line six parallels for treated and nine for non-treated cells were used, and readings for HEK293-6E were recorded at least in triplicates. Percent proliferation was derived as $[(OD_{450/620\ \text{test wells}} - OD_{450/620\ \text{background}})/(OD_{450/620\ \text{untreated control}} - OD_{450/620\ \text{background}})] \times 100$, means and SD are presented. Statistical analysis to discover the difference from non-treated control or VEGF-only control was performed with one-way ANOVA and multiple comparisons were done with post-hoc Holm-Bonferroni correction (at least $P < 0.05$ was considered the threshold for significance).

Internalization assay

100 µg of CX_AC*TRA_BCF and CX-CT6_AC*TRA-CT6_BCF at about 1 mg/ml were labeled with Molecular Probes® Alexa Fluor® 488 Antibody Labeling Kit (Thermo Fisher Scientific) exactly according to manufacturer's instructions, and used to treat A431 cells overnight at 66.6 nM with or without 200 nM $VEGF_{109}$N75Q in DMEM with 10% FBS and antibiotics in 1 ml-volume per well of a 12-well plate (Nunc) with 1×10^5 cells. Cells were then washed three times with PBS, scraped off and blocked with 2% BSA-PBS at 1×10^6 cells/ml

for 30 min on ice. After pelleting at 300 *g*, 5 min at 4 °C, 10^5 cells were resuspended in 100 µl anti-Alexa Fluor® 488 quenching antibody at 50 µg/ml (A11094, Thermo Fisher Scientific) and incubated for 30 min on ice, in parallel with non-quenched control samples in 2% BSA-PBS only. After centrifugation at 300 *g*, 5 min at 4 °C, the samples were resuspended in 200 µl ice-cold PBS and the fluorescence of 5000 events per sample was measured using Guava®easyCyte™ (Luminex). Duplicate measurements were performed.

Apoptosis assay with annexinV

A431 cells were seeded in 1 ml DMEM with 10% FBS and antibiotics at 1×10^5 cells/well in of a 12-well-plate. After overnight incubation at 37 °C, under 5% CO_2 in humidified atmosphere, they were incubated with 66.6 nM antibodies for 5 days. Centrifugation at 300 *g*, 4 °C for 5 min was used to harvest cells from the culture supernatant as well as the cells, detached with Cell Dissociation Buffer (Thermo Fisher Scientific) after two washes with PBS. Staining of 1×10^5 cells was done in 1 ml of AnnexinV-binding buffer (Thermo Fisher Scientific) containing 10 µl of the AnnexinV-Alexa Fluor™ 647 reagent (Thermo Fisher Scientific), and 1 µg/ml propidium iodide (PI) (Sigma-Aldrich) for 15 min at RT and the fluorescence was measured with Guava®easyCyte™ Flow Cytometer (Luminex) for duplicate samples. Percentage of only annexinV-positive cells (early apoptotic) and annexinV − as well as PI-positive cells (late apoptotic) was determined.

ADCC reporter assay

We used ADCC Reporter Bioassay (Promega, Madison, Wisconsin, United States), which informs on the competence of an antibody to activate gene transcription through the nuclear factor of activated T-cells (NFAT) pathway in the effector cells. These are engineered Jurkat cells, which stably express the FcγRIIIa receptor and an NFAT response element driving expression of luciferase.

Ten thousand MB-MDA-468 cells per well of a 96-well-plate were seeded in 100 µl DMEM with 10% FBS and antibiotics and kept at 37 °C, 5% CO_2, in humidified atmosphere overnight. Then medium was replaced with 25 µl RPMI containing 4% low-IgG serum (assay medium), 25 µl serial antibody dilution in assay medium (three-fold starting at 66.6 nM) and 25 µl engineered Jurkat- FcγRIIIa reporter cells in assay medium at a ratio of effector to target cells (E:T) of 7.5:1. After 5 h-incubation at 37 °C, plates were removed, 100 µl of luminescence substrate were added and the luminescent signal measured in a Tecan Sunrise microplate reader. Triplicate measurements were taken and EC_{50} values were calculated using Prism 5.0. Readings of wells with target cells incubated with effector cells (no antibody control) were at the level of the wells with effector cells only.

HUVEC proliferation assay

Telomerase reverse transcriptase-immortalized HUVEC cells (Evercyte, Vienna, Austria) were seeded in complete EndoUP2 medium (Evercyte) at a split ratio of 1:4 into a gelatin-coated 96-well plate and cultured for 48 h at 37 °C in humidified atmosphere with 5% CO_2. Cells were starved of VEGF for 48 h in medium without VEGF. Test protein preparations in 10-fold dilutions starting from 5.76 nM were incubated with basal medium with VEGF to a final concentration of 15 ng/ml for 2 h at 37 °C, and then cell culture medium was exchanged for the pre-incubated mixture. After 72 h-cultivation, the proliferation of HUVEC cells was determined using 3-(4,5-dimethylthiazol-2-yl)-2,5-diphenyltetrazolium bromide (MTT) reduction assay. Sample sizes were $n = 4$ for the incubation with Fab-arm exchanged antibodies and $n = 3$ for incubation with bevacizumab, ANG-CT6 and BEV-CT6 mAb^2 antibodies. Percent proliferation was determined as $[(A_{570/690\_treated\ wells} - A_{570/690\_starved\ wells})/(A_{570/690\_VEGF\text{-}wells} - A_{570/690\_starved\ wells})] \times 100$; means and SD are presented. Statistical analysis was performed using one-way ANOVA.

Acknowledgements: Mass spectrometry experiments were conducted at Mass Spectrometry Facility at Max Perutz Labs, Vienna. HUVEC proliferation assay was excellently performed by Evercyte GmbH.

Author contributions: All the authors have accepted responsibility for the entire content of this submitted manuscript and approved submission.

Research funding: The financial support by the Company F-star, Christian Doppler Society, Austrian Federal Ministry for Digital and Economic Affairs and the National Foundation for Research, Technology and Development is gratefully acknowledged. This project was supported by EQ-BOKU VIBT GmbH and BOKU Core Facility for Biomolecular and Cellular Analysis. FB was also supported by the PhD program BioToP (Biomolecular Technology of Proteins) funded by the Austrian Science Fund (FWF W1224).

Conflict of interest statement: The authors declare no conflicts of interest regarding this article.

References

Benedetti, F., Stracke, F., Stadlmayr, G., Stadlbauer, K., Rüker, F., and Wozniak-Knopp, G. (2021). Bispecific antibodies with Fab-arms

featuring exchanged antigen-binding constant domains. Biochem. Biophys. Rep. 26: 1–9.

Björkelund, H., Gedda, L., Barta, P., Malmqvist, M., and Andersson, K. (2011). Gefitinib induces epidermal growth factor receptor dimers which alters the interaction characteristics with 125I-EGF. PLoS One 6: 24739.

Blair, H.A. (2019). Emicizumab: a review in haemophilia A. Drugs 79: 1697–1707.

Bogen, J.P., Carrara, S.C., Fiebig, D., Grzeschik, J., Hock, B., and Kolmar, H. (2021). Design of a trispecific checkpoint inhibitor and natural killer cell engager based on a 2 + 1 common light chain antibody architecture. Front. Immunol. 12: 1–16.

Buchanan, A., Clementel, V., Woods, R., Harn, N., Bowen, M.A., Mo, W., Popovic, B., Bishop, S.M., Dall'Acqua, W., Minter, R., et al. (2013). Engineering a therapeutic IgG molecule to address cysteinylation, aggregation and enhance thermal stability and expression. MAbs 5: 255–262.

Dall'Acqua, W., Simon, A.L., Mulkerrin, M.G., and Carter, P. (1998). Contribution of domain interface residues to the stability of antibody CH_3 domain homodimers. Biochemistry 37: 9266–9273.

Edelman, G.M., Cunningham, B.A., Gall, W.E., Gottlieb, P.D., Rutishauser, U., and Waxdal, M.J. (1969). The covalent structure of an entire gamma G immunoglobulin molecule. Proc. Natl. Acad. Sci. U.S.A. 63: 78–85.

Gantke, T., Weichel, M., Herbrecht, C., Reusch, U., Ellwanger, K., Fucek, I., Eser, M., Müller, T., Griep, R., Molkenthin, V., et al. (2017). Trispecific antibodies for CD16A-directed NK cell engagement and dual-targeting of tumor cells. Protein Eng. Des. Sel. 30: 673–684.

Garcia, J., Hurwitz, H.I., Sandler, A.B., Miles, D., Coleman, R.L., Deurloo, R., and Chinot, O.L. (2020). Bevacizumab (Avastin®) in cancer treatment: a review of 15 years of clinical experience and future outlook. Cancer Treat. Rev. 86: 102017.

Garfall, A.L. and June, C.H. (2019). Trispecific antibodies offer a third way forward for anticancer immunotherapy. Nature 575: 450–451.

Gaspar, M., Pravin, J., Rodrigues, L., Uhlenbroich, S., Everett, K.L., Wollerton, F., Morrow, M., Tuna, M., and Brewis, N. (2020). CD137/OX40 bispecific antibody induces potent antitumor activity that is dependent on target coengagement. Cancer Immunol. Res. 8: 781–793.

Gauthier, L., Morel, A., Anceriz, N., Rossi, B., Blanchard-Alvarez, A., Grondin, G., Trichard, S., Cesari, C., Sapet, M., Bosco, F., et al. (2019). Multifunctional natural killer cell engagers targeting NKp46 trigger protective tumor immunity. Cell 177: 1701–1713.e16.

Grugan, K.D., Dorn, K., Jarantow, S.W., Bushey, B.S., Pardinas, J.R., Laquerre, S., Moores, S.L., and Chiu, M.L. (2017). Fc-mediated activity of EGFR x c-Met bispecific antibody JNJ-61186372 enhanced killing of lung cancer cells. MAbs 9: 114–126.

Hamma-Kourbali, Y., Starzec, A., Vassy, R., Martin, A., Kraemer, M., Perret, G., and Crépin, M. (2003). Carboxymethyl benzylamide dextran inhibits angiogenesis and growth of VEGF-overexpressing human epidermoid carcinoma xenograft in nude mice. Br. J. Cancer 89: 215.

Husain, B. and Ellerman, D. (2018). Expanding the boundaries of biotherapeutics with bispecific antibodies. BioDrugs 32: 441–464.

Kariolis, M.S., Wells, R.C., Getz, J.A., Kwan, W., Mahon, C.S., Tong, R., Kim, D.J., Srivastava, A., Bedard, C., Henne, K.R., et al. (2020). Brain delivery of therapeutic proteins using an Fc fragment blood-brain barrier transport vehicle in mice and monkeys. Sci. Transl. Med. 12, https://doi.org/10.1126/scitranslmed.aay1359.

Khan, K.A., Wu, F.T., Cruz-Munoz, W., and Kerbel, R.S. (2021). Ang2 inhibitors and Tie2 activators: potential therapeutics in perioperative treatment of early stage cancer. EMBO Mol. Med. 13, https://doi.org/10.15252/EMMM.201708253.

Kraman, M., Faroudi, M., Allen, N.L., Kmiecik, K., Gliddon, D., Seal, C., Koers, A., Wydro, M.M., Batey, S., Winnewisser, J., et al. (2020). FS118, a bispecific antibody targeting LAG-3 and PD-L1, enhances T-cell activation resulting in potent antitumor activity. Clin. Cancer Res. 26: 3333–3344.

Kut, C., Mac Gabhann, F., and Popel, A.S. (2007). Where is VEGF in the body? A meta-analysis of VEGF distribution in cancer. Br. J. Cancer 97: 978.

Labrijn, A.F., Meesters, J.I., De Goeij, B.E.C.G., Van Den Bremer, E.T.J., Neijssen, J., Van Kampen, M.D., Strumane, K., Verploegen, S., Kundu, A., Gramer, M.J., et al. (2013). Efficient generation of stable bispecific IgG1 by controlled Fab-arm exchange. Proc. Natl. Acad. Sci. U.S.A. 110: 5145–5150.

Labrijn, A.F., Meesters, J.I., Priem, P., de Jong, R.N., van den Bremer, E.T.J., van Kampen, M.D., Gerritsen, A.F., Schuurman, J., and Parren, P.W.H.I. (2014). Controlled Fab-arm exchange for the generation of stable bispecific IgG1. Nat. Protoc. 9: 2450–2463.

Labrijn, A.F., Janmaat, M.L., Reichert, J.M., and Parren, P.W.H.I. (2019). Bispecific antibodies: a mechanistic review of the pipeline. Nat. Rev. Drug Discov. 18: 585–608.

Lakins, M.A., Koers, A., Giambalvo, R., Munoz-Olaya, J., Hughes, R., Goodman, E., Marshall, S., Wollerton, F., Batey, S., Gliddon, D., et al. (2020). FS222, a CD137/PD-L1 tetravalent bispecific antibody, exhibits low toxicity and antitumor activity in colorectal cancer models. Clin. Cancer Res. 26: 4154–4167.

Leung, K.M., Batey, S., Rowlands, R., Isaac, S.J., Jones, P., Drewett, V., Carvalho, J., Gaspar, M., Weller, S., Medcalf, M., et al. (2015). A HER2-specific modified Fc fragment (Fcab) induces antitumor effects through degradation of HER2 and apoptosis. Mol. Ther. 23: 1722–1733.

Lobner, E., Humm, A.-S., Göritzer, K., Mlynek, G., Puchinger, M.G., Hasenhindl, C., Rüker, F., Traxlmayr, M.W., Djinović-Carugo, K., and Obinger, C. (2017a). Fcab-HER2 interaction: a ménage à trois. Lessons from X-ray and solution studies. Structure 25: 878–889.e5.

Lobner, E., Humm, A.-S., Mlynek, G., Kubinger, K., Kitzmüller, M., Traxlmayr, M.W., Djinović-Carugo, K., and Obinger, C. (2017b). Two-faced Fcab prevents polymerization with VEGF and reveals thermodynamics and the 2.15 Å crystal structure of the complex. MAbs 9: 1088–1104.

Moores, S.L., Chiu, M.L., Bushey, B.S., Chevalier, K., Luistro, L., Dorn, K., Brezski, R.J., Haytko, P., Kelly, T., Wu, S.J., et al. (2016). A novel bispecific antibody targeting EGFR and cMet is effective against EGFR inhibitor-resistant lung tumors. Cancer Res. 76: 3942–3953.

Neijssen, J., Cardoso, R.M.F., Chevalier, K.M., Wiegman, L., Valerius, T., Anderson, G.M., Moores, S.L., Schuurman, J., Parren, P.W.H.I., and Strohl, W.R., et al (2021). Discovery of amivantamab (JNJ-61186372), a bispecific antibody targeting EGFR and MET. J. Biol. Chem. 296: 1–13.

Newman, M.J. and Benani, D.J. (2016). A review of blinatumomab, a novel immunotherapy. J. Oncol. Pharm. Pract. 22: 639–645.

Nicolò, M., Ferro Desideri, L., Vagge, A., and Traverso, C.E. (2021). Faricimab: an investigational agent targeting the Tie-2/angiopoietin pathway and VEGF-A for the treatment of retinal diseases. Expert Opin. Investig. Drugs 30: 193–200.

Nie, S., Wang, Z., Moscoso-Castro, M., D'Souza, P., Lei, C., Xu, J., and Gu, J. (2020). Biology drives the discovery of bispecific antibodies as innovative therapeutics. Antib. Ther. 3: 18.

Pacchiana, G., Chiriaco, C., Stella, M.C., Petronzelli, F., de Santis, R., Galluzzo, M., Carminati, P., Comoglio, P.M., Michieli, P., and Vigna, E. (2010). Monovalency unleashes the full therapeutic potential of the DN-30 anti-met antibody. J. Biol. Chem. 285: 36149.

Pardridge, W.M. (2015). Blood-brain barrier drug delivery of IgG fusion proteins with a transferrin receptor monoclonal antibody. Expert Opin. Drug Deliv. 12: 207–222.

Schneider, D., Xiong, Y., Wu, D., Nölle, V., Schmitz, S., Haso, W., Kaiser, A., Dropulic, B., and Orentas, R.J. (2017). A tandem CD19/CD20 CAR lentiviral vector drives on-target and off-target antigen modulation in leukemia cell lines. J. Immunother. Cancer 5: 42.

Sellmann, C., Doerner, A., Knuehl, C., Rasche, N., Sood, V., Krah, S., Rhiel, L., Messemer, A., Wesolowski, J., Schuette, M., et al. (2016). Balancing selectivity and efficacy of bispecific epidermal growth factor receptor (EGFR) x c-MET antibodies and antibody-drug conjugates. J. Biol. Chem. 291: 25106–25119.

Shi, S.Y., Lu, Y.-W., Liu, Z., Stevens, J., Murawsky, C.M., Wilson, V., Hu, Z., Richards, W.G., Michaels, M.L., Zhang, J., et al. (2018). A biparatopic agonistic antibody that mimics fibroblast growth factor 21 ligand activity. J. Biol. Chem. 293: 5909–5919.

Steinmetz, A., Vallée, F., Beil, C., Lange, C., Baurin, N., Beninga, J., Capdevila, C., Corvey, C., Dupuy, A., Ferrari, P., et al. (2016). CODV-Ig, a universal bispecific tetravalent and multifunctional immunoglobulin format for medical applications. MAbs 8: 867–878.

Strohl, W.R. and Naso, M. (2019). Bispecific T-cell redirection versus chimeric antigen receptor (CAR)-T cells as approaches to kill cancer cells. Antibodies 8: 1–68.

Strop, P., Ho, W.H., Boustany, L.M., Abdiche, Y.N., Lindquist, K.C., Farias, S.E., Rickert, M., Appah, C.T., Pascua, E., Radcliffe, T., et al. (2012). Generating bispecific human IgG1 and IgG2 antibodies from any antibody pair. J. Mol. Biol. 420: 204–219.

Ulitzka, M., Carrara, S., Grzeschik, J., Kornmann, H., Hock, B., and Kolmar, H. (2020). Engineering therapeutic antibodies for patient safety: tackling the immunogenicity problem. Protein Eng. Des. Sel. 33: 1–12.

Vallera, D.A., Felices, M., McElmurry, R., McCullar, V., Zhou, X., Schmohl, J.U., Zhang, B., Lenvik, A.J., Panoskaltsis-Mortari, A., Verneris, M.R., et al. (2016). IL15 trispecific killer engagers (TriKE) make natural killer cells specific to $CD33^{+}$ targets while also inducing persistence, *in vivo* expansion, and enhanced function. Clin. Cancer Res. 22: 3440–3450.

von Kreudenstein, T.S., Escobar-Carbrera, E., Lario, P.I., D'Angelo, I., Brault, K., Kelly, J., Durocher, Y., Baardsnes, J., Jeremy Woods, R., Xie, M.H., et al. (2013). Improving biophysical properties of a bispecific antibody scaffold to aid developability: quality by molecular design. MAbs 5: 646–654.

Wang, N., Patel, H., Schneider, I.C., Kai, X., Varshney, A.K., and Zhou, L. (2021). An optimal antitumor response by a novel CEA/CD3 bispecific antibody for colorectal cancers. Antib. Ther. 4: 90–100.

Wozniak-Knopp, G., Bartl, S., Bauer, A., Mostageer, M., Woisetschläger, M., Antes, B., Ettl, K., Kainer, M., Weberhofer, G., Wiederkum, S., et al. (2010). Introducing antigen-binding sites in structural loops of immunoglobulin constant domains: Fc fragments with engineered HER2/neu-binding sites and antibody properties. Protein Eng. Des. Sel. 23: 289–297.

Wozniak-Knopp, G., Stadlmayr, G., Perthold, J.W., Stadlbauer, K., Woisetschläger, M., Sun, H., and Rüker, F. (2017). Designing Fcabs: well-expressed and stable high affinity antigen-binding Fc fragments. Protein Eng. Des. Sel. 30: 567–581.

Wu, L., Seung, E., Xu, L., Rao, E., Lord, D.M., Wei, R.R., Cortez-Retamozo, V., Ospina, B., Posternak, V., Ulinski, G., et al. (2020). Trispecific antibodies enhance the therapeutic efficacy of tumor-directed T cells through T cell receptor co-stimulation. Nat. Can. 1: 86–98.

Wu, X. and Demarest, S.J. (2019). Building blocks for bispecific and trispecific antibodies. Methods 154: 3–9.

Supplementary Material: The online version of this article offers supplementary material (https://doi.org/10.1515/hsz-2021-0376).